Research Article

Detection of Water Vapor in Halley's Comet

MICHAEL J. MUMMA, HAROLD A. WEAVER, HAROLD P. LARSON, D. SCOTT DAVIS, MICHAEL WILLIAMS

Gaseous, neutral H_2O was detected in the coma of comet Halley on 22.1 and 24.1 December 1985 Universal Time. Nine spectral lines of the ν_3 band (2.65 micrometers) were found by means of a Fourier transform spectrometer ($\lambda/\Delta\lambda \sim 10^5$) on the NASA-Kuiper Airborne Observatory. The water production rate was $\sim 6 \times 10^{28}$ molecules per second on 22.1 December and 1.7×10^{29} molecules per second on 24.1 December UT. The numbers of spectral lines and their intensities are in accord with nonthermal-equilibrium cometary models. Rotational populations are derived from the observed spectral line intensities and excitation conditions are discussed. The ortho-para ratio was found to be 2.66 ± 0.13, corresponding to a nuclear-spin temperature of 32 K (+5 K, −2 K), possibly indicating that the observed water vapor originated from a low-temperature ice.

According to Whipple's "dirty-snowball" model, the cometary nucleus is a fragile, solid body, an agglomeration of dust and frozen gases (*1*). Vaporization causes the nucleus to lose several meters of thickness on each perihelion passage, exposing fresh material on successive apparitions. Halley's comet has made 29 passages (*2*) since its first appearance in recorded history, and the material exposed today was once buried deep within the nucleus, far below the original surface layer where significant chemical modification by long-term cosmic ray exposure could have occurred (*3*). The material currently being evolved from the nucleus is thought to be primordial, unmodified since condensing from its natal cloud of gas and dust, possibly the presolar nebula or an interstellar cloud. The composition of the nucleus is the fingerprint of that nebula, a "Rosetta-stone," from which we can determine its physics and chemistry. For this reason, the identification of these parent molecular ices and quantitative measurements of their abundances are central problems in cometary research.

The composition of the volatile fraction has been estimated based on arguments derived from our current understanding of interstellar chemistry (*4*), on models of the presolar nebula (*5*), and on inferences drawn from the dissociation by-products as revealed by cometary spectra (*6*). The models indicate that the dominant ice should be ordinary H_2O, and strong circumstantial evidence supports this expectation. Indeed, a spectral feature attributed to water ice has been reported in two comets (*7, 8*) observed at large heliocentric distance; but abundance estimates have not been established, and the identification has itself been challenged (*9*).

Atomic hydrogen (H), oxygen (O), and the hydroxyl radical (OH) are laboratory photodissociation products of H_2O that have been observed simultaneously in ultraviolet spectra of several comets (*10*), and OH has been observed at radio wavelengths as well (*11*). The relative abundances and spatial distributions of these species are consistent with a common H_2O source for all of them, but model uncertainties (for example, poor knowledge of the intensity of the exciting solar flux in the case of O, and incomplete treatment of radiative transfer in the case of H and O) prevent us from making a definitive link to H_2O.

The ion H_2O^+, first identified (*12*) spectroscopically in comets in 1974, is now routinely studied from ground-based observatories, and it was recently measured directly by a plasma spectrometer (*13*) on the International Cometary Explorer spacecraft, which flew through comet Giacobini-Zinner in September 1985. Unfortunately, H_2O cannot be established unambiguously as the parent of H_2O^+, since ionization processes in comets are poorly understood.

Earlier spectroscopic attempts to detect water vapor directly have concentrated on its rotational spectral lines at radio wavelengths, since it has no known stable electronic transitions in the ultraviolet or visible spectral regions, and its strong infrared vibrational and rotational transitions are obscured by corresponding absorptions of terrestrial atmospheric water. Consequently, only the radio maser transitions were available for ground-based searches. Marginal detections of the 6_{16}–5_{23} line (near 22 GHz) (see legend to Fig. 1) were reported in comet Bradfield 1974III (*14*) and later in comet IRAS-Araki-Alcock 1983d (*15*), but other comets failed to show this line. Furthermore, quantitative production rates could not be derived since the excitation mechanisms are not understood.

The generally disappointing results of radio searches (*16*) for the parent molecules, and advances in infrared technology, led to searches for infrared vibrational emissions from methane (*17*) and ammonia (*18*) in comet Kohoutek, and to a general survey of comet West at wavelengths from 0.9 to 2.5 μm (*19*), but no parent molecular emissions were identified. This prompted careful theoretical considerations of the non-LTE (local thermodynamic equilibrium) environment of the cometary coma, and of the mechanisms for producing infrared vibrational emissions (*20*). Preliminary calculations of infrared fluorescence efficiencies (g factors) (*21*) gradually evolved into more sophisticated treatments which explicitly considered the unusual excitation conditions expected in cometary comae (*22, 23*). The new models guided the observational searches by identifying which experimental techniques were most likely to succeed. The most promising band was the asymmetric stretch

M. J. Mumma is head of the Planetary Systems Branch, Code 693, Goddard Space Flight Center, Greenbelt, MD 20771. H. A. Weaver is an associate research scientist at the Center for Astrophysical Sciences, Johns Hopkins University, Baltimore, MD 21218. H. P. Larson and M. Williams are members of the Lunar and Planetary Laboratory, University of Arizona, Tucson, AZ 85721. D. S. Davis is a research associate at the Steward Observatory, University of Arizona, Tucson, AZ 85721.

vibration (ν_3) of H_2O, near 2.65 µm. Observations from airplane altitudes were shown to be necessary, thereby avoiding absorption by atmospheric water vapor (*22*). These theoretical models also led to ground-based searches for weak intercombination vibrational bands of H_2O (101 and 011, near 1.4 µm, and 1.9 µm, respectively), resulting in a reported "probable detection" of H_2O in comet Halley (*24*).

We report here the search for and detection of nine lines in the ν_3 band of H_2O in comet Halley, confirming that water vapor is a major component of the cometary coma, and demonstrating that infrared resonance fluorescence is a powerful new tool for cometary research.

Infrared fluorescence excitation in H_2O. The water molecule is an asymmetric rotor and, being strongly polar, possesses intense vibrational bands (ν_2, ν_3) and a strong rotational spectrum. Some energy levels and rotational-vibrational transitions important for studying the cometary problem are shown in Fig. 1. In thermal equilibrium at 300 K, all of the rotational levels shown (in the lowest vibrational state) (Fig. 1), and many others, are significantly populated so that the infrared ν_3 band (001–000) consists of hundreds of individual spectral lines. Several of these are indicated (Fig. 1). However, owing to the extremely low number densities prevailing throughout most of the coma, collisions there are not frequent enough to keep the rotational population equilibrated (except possibly within 1000 km of the nucleus, where fewer than 1 percent of the coma H_2O molecules should be found). Hence the rotational population relaxes radiatively until only the lowest few levels in the ortho and para configurations are significantly occupied. The numbers of spectral lines are correspondingly reduced, but their fluorescence efficiencies are greatly enhanced because of the increased fractional population in the remaining occupied levels. Theoretical details and quantitative predictions have been described (*22, 23*).

According to Weaver and Mumma (*22*), the specific intensity of the cometary H_2O lines should exceed the continuum level near 2.65 µm by several orders of magnitude, but only five strong lines would be produced if the H_2O were fully relaxed to the lowest ortho and para levels (1_{01} and 0_{00}, respectively). Models that include radiative trapping of rotational spectral lines (*25*) show that the collision-dominated regime is extended to somewhat lower densities than are predicted for the optically thin case, with a corresponding increase in the number of predicted lines.

Lunar and cometary observations. The few predicted cometary emission lines in the ν_3 band would be hopelessly obscured by saturated atmospheric H_2O lines at even the driest ground-based sites (see footnote to Table 1). Special high-altitude observatories, or spaceborne facilities, are therefore required to search for them. Acceptable observations can be made from aircraft operating at altitudes near or above the tropopause, where the water vapor column abundance is often ~100-fold lower. However, the stronger atmospheric H_2O lines remain optically thick even at these altitudes, requiring that the observations be made at a time when the comet's geocentric velocity shifts its lines sufficiently far from the residual terrestrial H_2O lines.

The data reported here were obtained aboard NASA's Kuiper

Table 1. Observing log during December 1985.

Object	Ephemeris* R	Ephemeris* Δ	Ephemeris* $\dot{\Delta}$	Observing period (UT)	Flight altitude (km)	Terrestrial H_2O (pr. µm)†
Comet Halley	1.16	0.96	34.97	22.10–.15	11.3–12.5	15
Moon				22.16–.19	12.5	26
α Ursae Minoris				23.21–.23	12.5	8
α Aurigae				23.24–.26	12.5	11
Comet Halley	1.13	1.00	35.11	24.10–.15	12.5	30
Moon				24.16–.18	12.5	26
α Ursae Minoris				24.19–.22	12.5	36

*R, heliocentric distance (AU); Δ, geocentric distance (AU); $\dot{\Delta}$, Radial component of geocentric velocity (kilometers per second). †Precipitable micrometer, pr. µm. One precipitable micrometer represents the column density of atmospheric water vapor which, if condensed, would form a layer of liquid water 1 µm thick. The driest ground-based observatories generally experience atmospheric water burdens of ≥1 precipitable millimeter.

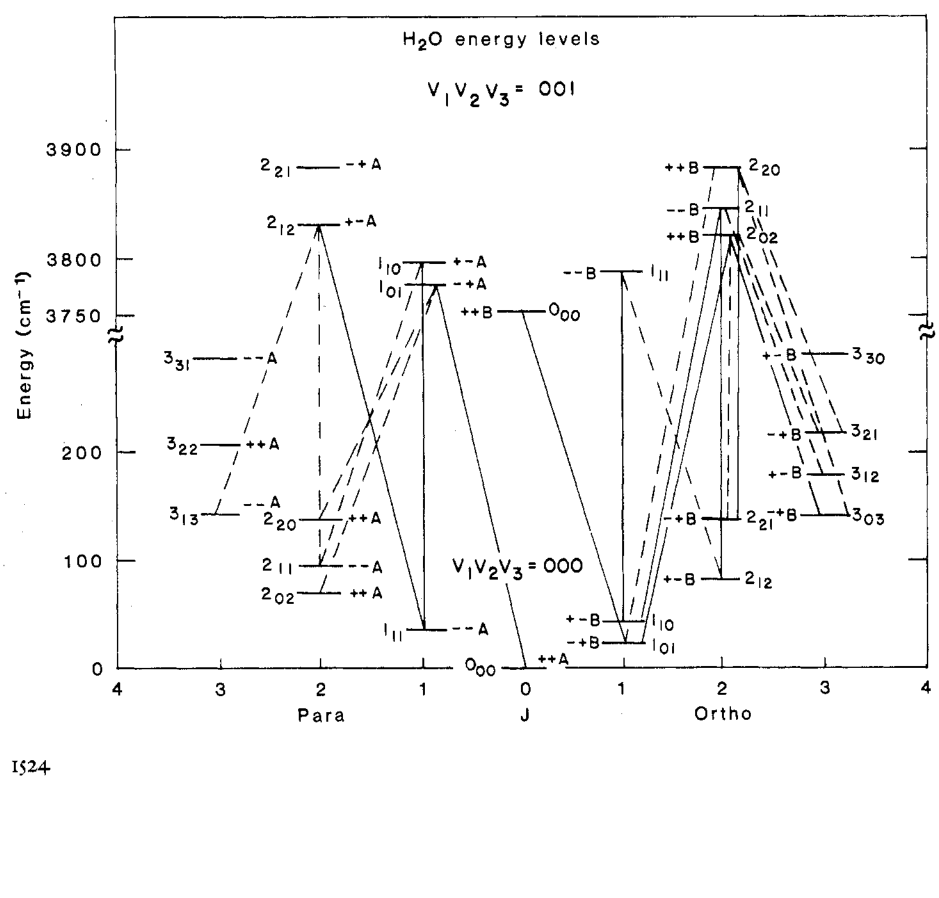

Fig. 1. Energy level diagram for H_2O, showing some rotational levels in the 000 and the 001 vibrational states. V_1, V_2, V_3 are vibrational quantum numbers for the normal modes ν_1, ν_2, ν_3 [see (*27*)]. Individual levels are labeled with their rotational quantum numbers (J, K_a, K_c) and the parameters (−, +, A, B) [see (*27*)]. The transitions detected in comet Halley are shown as solid lines (for example, 1_{11}–1_{01}) and the (unobserved) accompanying branching transitions are shown by dashed lines (for example, 1_{11}–2_{12}). The ortho transition (2_{02}–3_{03}) was detected in a survey spectrum taken on 24 December. Only the lowest few levels in each of the ortho- and para-modifications are significantly occupied. The transition (6_{16}–5_{23}), belonging to ortho-H_2O, has been reported (*14, 15*) at radio wavelengths but is not expected to be present in comets if present models are correct.

Table 2. Spectrometer characteristics.

Factor	Description
Type	Fourier transform; step and integrate [see (*26*)]
Optical configuration	Dual input–dual output
Separation of input beams	11 arc minutes
Field of view (each beam)	41-arc-second diameter
Spectral resolution achieved	0.041 cm^{-1} (unapodized)
Velocity resolution	3.2 km sec^{-1} at 3800 cm^{-1}
Spectral bandwidth	2.61 to 2.71 μm (the 10 percent transmittance points)
Detectors	Indium antimonide (InSb), 0.5-mm diameter, 63 K

Airborne Observatory (KAO) with the University of Arizona high resolution Fourier transform spectrometer (FTS) (*26*). A log of the observations is given in Table 1. Some of the spectrometer's characteristics are listed in Table 2, including those that were specially selected to optimize the cometary observations. Telescope tracking was maintained with nearby field stars, if available, or with the comet itself. Frequent guiding checks were made to compensate for cometary drift and telescope field rotation. The tropopause was unseasonably high during these flights, varying from 11.3 to 14.3 km. This resulted in residual H_2O vapor along the line of sight that was two to three times normal values, which are typically ≤ 10 precipitable micrometers of H_2O. However, the terrestrial H_2O absorption, and its variations, had little effect on the cometary spectra because the large geocentric velocity of the comet ($\sim +35$ km sec^{-1}) shifted the cometary H_2O emission lines to the far red wings of the corresponding telluric H_2O absorption lines (see Figs. 2 and 3 for details).

Spectra of comet Halley and the Moon were acquired on 22 December and 24 December UT (Table 1). The spectra acquired on 24 December are shown in Fig. 2. Nine lines of H_2O were clearly detected in the cometary spectrum, Doppler-shifted toward lower frequencies ($\Delta\nu \sim -0.43$ cm^{-1}) with respect to the corresponding terrestrial lines. Three lines (P) belong to para H_2O and six lines (O) belong to ortho H_2O, and they are labeled by the quantum numbers (J, K_a, K_c) of the upper and lower energy states, respectively (*27*). Every transition which is expected is seen, and no extra lines are found. The observed transitions are shown as solid lines in Fig. 1, while transitions that are implied by known branching ratios are shown by dashed lines. In every case, those unobserved transitions occur at wavelengths where the atmosphere is opaque, even at KAO flight altitudes. Comparison with an H_2O atlas (*28*) shows that more than 100 additional ν_3 lines ($J < 12$) fall within our bandpass (Fig. 2), and more than 50 of those correspond to $J < 7$. However, none of these is seen in the cometary spectrum, confirming that the cometary H_2O is rotationally relaxed. The lunar spectrum reveals the presence of many atmospheric H_2O lines, and also the very strong CO_2 band (10°1–00°0) centered near 3716 cm^{-1} and extending to ~ 3750 cm^{-1}. It is evident by inspection that far fewer H_2O lines are seen in the cometary spectrum compared with the terrestrial case, as predicted by models of nonthermal equilibrium (*22, 23, 25*).

A particular virtue of Fourier transform spectroscopy is that it provides highly accurate frequency positions for the spectral lines. A typical line profile (1_{01}–0_{00}) is shown in Fig. 3. This presentation of the spectrum resulted from phase-correction of the interferograms, followed by Fourier sine transformation. The procedure resulted in a minimum width of the instrumental line shape, hence a maximum resolution of the cometary H_2O features. The apparent cometary H_2O line positions, their nucleocentric values (after removing the effects of the earth's rotation and geocentric cometary motion), and the laboratory rest frequencies are presented in Table 3. The observed and nucleocentric H_2O frequencies are reported only to 0.01 cm^{-1} at this time (final evaluation of errors is pending). Our preliminary analysis indicates that the H_2O lines are not significantly Doppler-shifted (at the 0.2 km sec^{-1} level) relative to the cometary nucleus. The cometary H_2O line profiles are unresolved at the instrumental velocity resolution of 3.2 km sec^{-1}.

The relative intensities of the cometary H_2O lines, corrected for atmospheric transmittance, are given in Table 3 for the spectrum

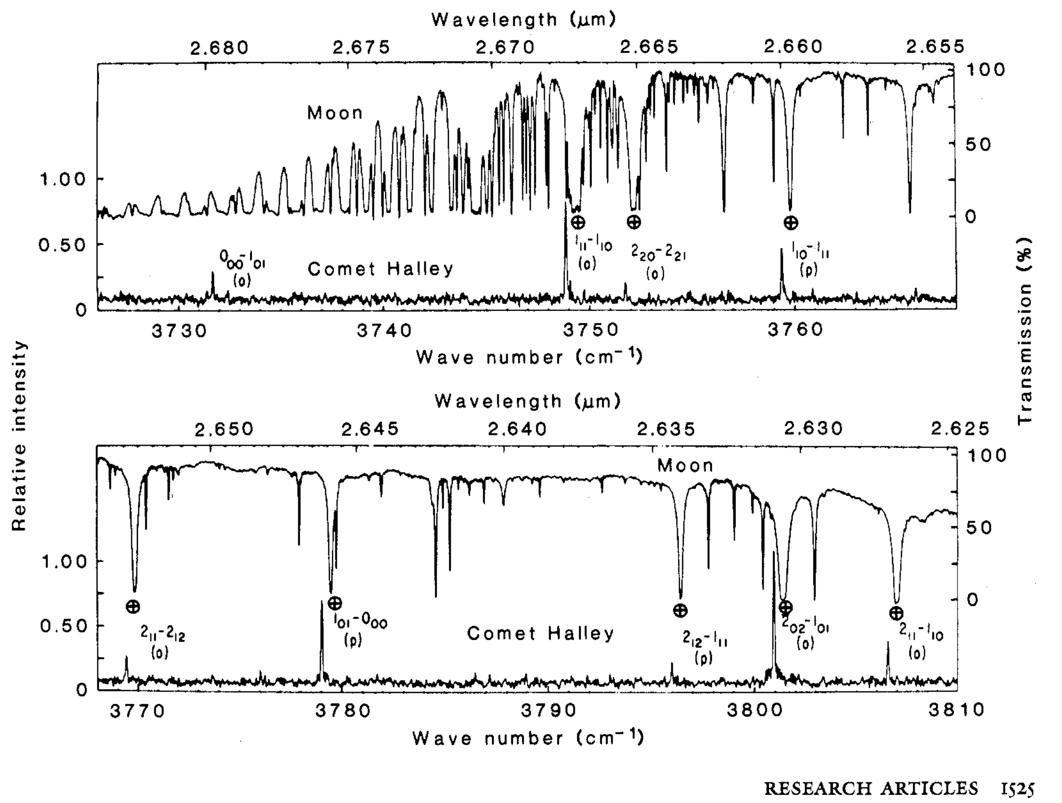

Fig. 2. H_2O emission in comet Halley measured on 24.10 December 1985. The observed spectrum reveals nine emission lines assigned to the ν_3 band of gaseous, neutral H_2O. Each line is labeled with the quantum numbers of the upper and lower states, and the letters in parentheses distinguish between ortho- and para-H_2O transitions. The displayed spectra are uncorrected for atmospheric transmission and instrumental response. The mean offset in the baseline is not continuum flux from the comet, but an artifact of the power spectrum calculation used for this presentation of the data. The lunar reflectance spectrum allows calibration of the relative intensities of the cometary H_2O features (Table 3). The residual terrestrial absorptions at aircraft altitude include CO_2 ($\lambda > 2.67$ μm) and H_2O. The telluric H_2O absorption lines that correspond to the Doppler-shifted cometary H_2O emission lines are marked with the symbol ⊕. Cometary H_2O emission does not accompany every strong telluric H_2O feature; this is a consequence of rotational relaxation in the coma.

Table 3. Comet Halley H_2O: observed frequencies and intensities. A tenth line (ortho 2_{02}–3_{03}; rest frequency, 3688.453 cm^{-1}) was detected in a survey spectrum taken on 24 December.

H_2O line frequencies				Relative intensities‖	
Transition*	Observed†	Nucleocentric‡	Rest§	22.10 Dec.	24.10 Dec.
2_{11}–1_{10}	3806.58	3807.02	3807.014	33 ± 7	36.5 ± 2.6
2_{02}–1_{01}	3800.98	3801.43	3801.420	100 ± 7	100.0 ± 1.8
2_{12}–1_{11}	3796.00	3796.44	3796.440		14.7 ± 1.8
1_{01}–0_{00}	3779.05	3779.50	3779.493	52 ± 5	41.2 ± 1.7
2_{11}–2_{12}	3769.45	3769.90	3769.890		15.7 ± 1.6
1_{10}–1_{11}	3759.41	3759.85	3759.845	25 ± 4	24.4 ± 1.5
2_{20}–2_{21}	3751.77	3752.21	3752.213		13.5 ± 1.8
1_{11}–1_{10}	3748.89	3749.33	3749.331	52 ± 6	67.0 ± 2.9
0_{00}–1_{01}	3731.70	3732.14	3732.135	103 ± 28	68.4 ± 14.1

*The quantum numbers of the upper and lower levels, $J'K_a'K_c'$ to $J''K_a''K_c''$. See (27). †Comet Halley, observed absolute frequency after applying instrumental corrections to the spectrum of 24.10 December. ‡Comet Halley, after removing geocentric and topocentric corrections. §Rest frequencies (32). Absolute accuracy is better than 0.003 cm^{-1} and relative accuracy is higher. ‖Relative intensities for each day are normalized to that of the 3801 cm^{-1} transition. Absolute intensities were about three times larger on 24.10 December relative to 22.10 December. All errors are $\pm 1\sigma$.

shown in Fig. 2. We found the comet to be brighter by a factor of about 3 on 24 December UT, when compared with that on 22 December. We have not detected the cometary continuum. Based on extrapolations from ground-based continuum observations (29), the ratio of specific intensities for our brightest line (3801 cm^{-1}) and the nearby cometary continuum should be ~600 to 1, whereas our achieved signal-to-noise ratio on the line was ~41 in the power spectrum (Fig. 2) and ~55 in the phase-corrected, transformed spectrum (Table 3). We would therefore not expect to have detected the continuum.

Water production rate. The relative intensities were converted to absolute units in order to make a direct estimate of the H_2O production rate. This provisional calibration is based on the nominal noise-equivalent spectral radiance (NESR) of our spectrometer. The

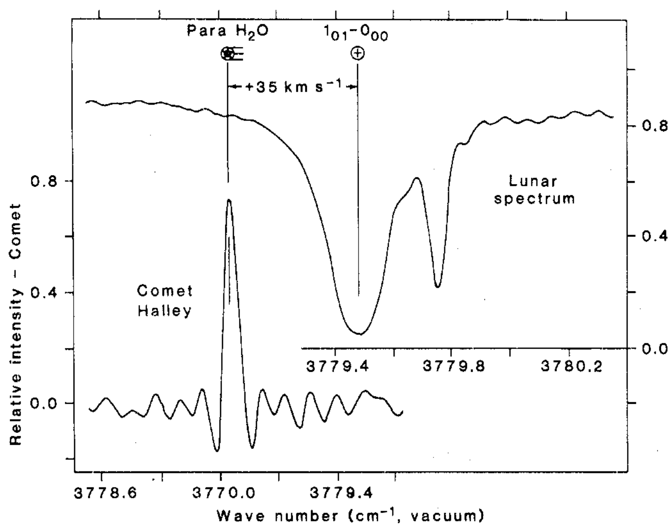

Fig. 3. An example of the H_2O emission line profile in comet Halley measured on 24.10 December 1985. The observed line profile (1_{01}–0_{00}) is similar to a sinc function, the theoretical instrumental line shape for a Fourier transform spectrometer. The first, strong negative side lobes are evident, but the noise level masks weaker artifacts of this line shape. The lunar spectrum is also shown, and the large (~+35 km sec^{-1}) geocentric Doppler shift of the cometary line is indicated. The width and nucleocentric Doppler shift of the cometary line relate to the magnitude and distribution of the H_2O velocity field in the coma.

signal-to-noise ratios achieved during observations of two calibration stars (α Ursae Minoris and α Aurigae in Table 1) confirm this nominal instrument sensitivity to within a factor of about 2. A final absolute calibration will be available from our observations after perihelion in late March 1986.

The intensities of the unobserved transitions (dashed lines in Fig. 1) were calculated from those of the detected lines and with the use of branching ratios derived from known line strengths (28), in order to obtain an estimate for the total ν_3 band intensity. This procedure should give a reasonably accurate value for the total band intensity, since contributions from higher lying rotational levels are expected to be small, as discussed earlier. Using the absolute calibration discussed above, we find

$$I_{\text{total}} = 6.9 \times 10^{-10}\ \text{W cm}^{-2}\ \text{sr}^{-1}$$

of which the detected transitions contribute 45 percent.

The number of water molecules in our beam may be estimated from

$$N_{H_2O} = \frac{I_{\text{total}}}{g_{\text{band}} hc\nu}\ \pi^2 \Delta^2 \theta_b^{\,2}$$

where Δ is the geocentric distance (cm), θ_b is the beam diameter (radians), ν is the photon frequency (cm^{-1}), and g_{band} is the solar fluorescence efficiency (photons molecule^{-1} sec^{-1}) for the entire band (see 22). Using $g_{\text{band}} = 2.1 \times 10^{-4}$, at heliocentric distance R = 1.13 AU (astronomical units), we find

$$N_{H_2O} = 3.7 \times 10^{33}\ \text{molecules}$$

in our beam. A simple Haser model (spherical symmetry, uniform radial outflow velocity, 0.8 km sec^{-1}; H_2O dissociation lifetime, 10^5 seconds at 1.13 AU) shows that 22 percent of the H_2O molecules in the coma will be sampled by our beam (diameter, 41 arc seconds). Optical thickness effects become important for the stronger ν_3 lines within 1000 km of the nucleus, but fewer than 1 percent of the total H_2O inventory should reside there, affecting our derived H_2O production rate by no more than 4 percent. We find

$$Q_{H_2O} = \frac{4.5\ N_{H_2O}}{\tau} = 1.7 \times 10^{29}\ \text{molecules sec}^{-1}$$

on 24.1 December UT and $Q_{H_2O} \sim 4 \times 10^{28}$ sec^{-1} on 22.1 December 1985 UT.

Ortho-para ratio. Let us now compare the total ortho-H_2O emission intensities with the total para-H_2O intensities. It is exceedingly difficult to convert molecules with one nuclear spin alignment to the other (30). Mumma (31) has suggested that this may be used to good advantage in comets, by regarding the nuclear spin temperature as being characteristic of the origin of the observed H_2O. Thus, if the H_2O were sublimated from the ice phase, its nuclear spin temperature (defining the ortho-para ratio) should be characteristic of the physical temperature of the ice. If the H_2O were produced by reactive gas-phase chemistry (or dissociation of a precursor molecule), then the ortho-para ratio should reflect the numbers of final states available, that is, 3 to 1. Central to this concept is the argument that the newly liberated H_2O molecule experiences too few collisions to change its nuclear spin alignment, and that the ortho-para ratio remains unchanged throughout the coma.

From our relative intensities on 24.10 December, we find the ortho-para ratio to be

$$\frac{N_{\text{ortho}}}{N_{\text{para}}} = 2.66 \pm 0.13$$

The dependence of the ortho-para ratio on temperature may be calculated for water molecules in thermal equilibrium from the usual Boltzmann expression, accounting for nuclear spin statistics and rotational statistics properly and summing over the rotational states in the ortho- and para-manifolds separately (*27*). Then the temperature at which the cometary water vapor was last equilibrated may be determined by comparing the observed ortho-para ratio with the calculated ones. We find that the measured ortho-para ratio in Halley's comet corresponds to a nuclear spin temperature (T_{spin}) of

$$T_{spin} = 32\ K\ (+5\ K,\ -2\ K)$$

The range of nuclear spin temperatures is 28 to 45 K at the 95 percent confidence limit, which seems to support vaporization from a low-temperature ice as the major source of the observed H_2O. Comet Halley's equilibrium temperature at aphelion depends on its albedo, and ranges from 27 to 53 K for albedos from 0.9 to 0.05, respectively. Since the surface temperature is thought to reach ~200 K at 1 AU, the low value observed for the nuclear spin temperature suggests that accommodation of the ortho-para ratio to the higher temperature is incomplete. It is also possible that formation of icy grains in the inner coma may quench the nuclear spin temperature to low values. Although the present data are suggestive, further laboratory work will be needed to establish a rigorous connection between the observed nuclear spin temperatures and the physical temperature of the ice phase.

Furthermore, unrecognized errors in the measurement of individual line intensities could affect the derived ortho-para ratio significantly. This could be particularly serious for the 0_{00}–1_{01} ortho line, which exhibits a measured intensity smaller by a factor of 2.2 than expected (see Rotational populations). We do not see any specific reason to suspect the measured value, but if the observed intensity were replaced by the value expected for model B, then the ortho-para ratio would become 3.0. Other uncertainties could also lead to modification in the derived ortho-para ratio (for example, optical depth effects in the coma and incomplete information on the rotational distributions and on other excitation mechanisms for the ν_3 band).

Rotational populations. The line-by-line intensities (Table 3) may also be used to derive beam-averaged rotational populations in the ground vibrational state for comparison with models of the coma. A complete treatment of this problem is beyond the scope of this article; however, we present several preliminary solutions based on some simplifying assumptions. Fluorescence equilibrium is invoked for each observed rotational level in the vibrational state 001 (five levels for ortho-H_2O, three for para-H_2O). Rotational transitions within 001 are neglected, since $A_{rot} << A_{vib}$. Cascade into 001 from higher vibrational states is neglected, and the ν_3 lines are assumed to be optically thin.

Six lines of ortho-H_2O were observed, originating from five rotational levels in 001. Five rotational populations in the 000 vibrational state may be determined with the use of steady-state equations for these levels. Although the five upper levels are coupled to (pumped by) seven lower levels, two of the latter (3_{21} and 3_{12}) are expected to have very small rotational populations, owing to rapid rotational relaxation. Neglecting infrared pumping from these two levels permits us to determine the populations of the remaining five levels in 001, regardless of any further considerations (such as optical trapping, collisions, and pumping by ν_2 fluorescence) (Table 4, model A).

The population for 3_{03} is surprisingly large. We note that the expected intensity (*22*) of 0_{00}–1_{01} is 1.47, relative to 2_{02}–1_{01}, but the observed ratio is 0.68. Thus the 0_{00}–1_{01} line is more faint than expected by a factor of ~2.2. This requires a much larger pumping rate for 2_{02}—forcing a larger population in 3_{03}, and indeed requiring an inverted population with respect to 2_{12}. The rotational transition probability for 3_{03}–2_{12} is so large [$A_{rot} \sim 5.2(-2)\ sec^{-1}$] that no significant steady-state population is expected in 3_{03}. A seven-level solution (steady-state equations are incorporated for 3_{21} and 3_{12}) confirms the five-level results shown as model A, but also gives negligible population in 3_{21} and 3_{12}, demonstrating that the relative populations do not continue to increase with the inclusion of higher J levels. Thus the large population in 3_{03} cannot be due to the omission of 3_{21} and 3_{12} in model A. Model A seems to require a large unidentified pump into 2_{02} or 3_{03}, or some mechanism for reducing the intensity of 0_{00}–1_{01}.

Table 4. Beam-averaged rotational populations for H_2O in comet Halley.

Type	Model* A	Model* B	Model* C
	Ortho-H_2O		
1_{01}	23.7 ± 4.9†	59.8 ± 1.8	
1_{10}	29.1 ± 4.7	33.9 ± 5.2	
2_{12}	4.3 ± 14.6	5.3 ± 8.7	
2_{21}	3.4 ± 0.5	3.1	
3_{03}	39.4 ± 6.8		
	Para-H_2O		
0_{00}			55.9 ± 5.4
1_{11}			44.1

*Models A, B, C are described in the text. Model B is preferred for the ortho species (see text). †Errors represent propagated statistical uncertainties (±1σ) associated with the measured relative intensities (Table 3), with the relative absorption line strengths [~1 percent (*28*)], and with the branching ratios (~1.2 percent).

Independent information on the population of the 3_{03} level can be obtained by looking for other transitions in our passband which are pumped from 3_{03}. The absence of the 3_{22}–3_{21} transition at 3744.511 cm^{-1} allows us to place an upper limit (3σ) on the fractional population of 3_{03} at ≤ 0.09. This is considerably smaller than the model A result and is evidence that the reported intensity for the 0_{00}–1_{01} line may be incorrect, or that the model is incomplete.

The 0_{00}–1_{01} line lies between two strong (R22, R24) CO_2 lines in the 10°1 band, but plausible errors in the CO_2 interline opacity can at most account for ten's of percent error. Comparison of our line spectrum with atmospheric line atlases demonstrates good agreement, but if an unresolved stratospheric line were present, it might cause significant error in the measured intensity of the 0_{00}–1_{01} transition. We therefore solved a four-level model (omitting the 0_{00} level in $\nu_3 = 1$, and forcing $n_{303} = 0$), with the results given (Table 4, model B). The results are more in accord with theoretical expectations (*22*), and with the observed absence of the 3_{22}–3_{21} line; however, the intensity predicted for 0_{00}–1_{01} is 2.2 times larger than that observed (Table 3).

Both models show large populations in 1_{10} relative to 1_{01}, contrary to the earlier expectations (*22, 23*). Collisions are not expected to play an important role for the majority of molecules in our beam, thus collisional excitation of 1_{01} seems unlikely. The level 1_{10} can be radiatively pumped in the ν_3 band by the following sequence: (ν_3 pump, 1_{01}–2_{02}; cascade, 2_{02}–3_{03}; relaxation, 3_{03}–2_{12}; ν_3 pump, 2_{12}–1_{11}; cascade, 1_{11}–1_{10}). The rotational transition 2_{12}–1_{01} must be optically thick ($\tau \sim 7$) for this mechanism to operate efficiently, and two infrared pumping events are needed. A more efficient mechanism for pumping 1_{10} is by ν_2 band transitions (ν_2 pump 1_{01}–1_{10}; ν_2 cascade 1_{10}–2_{21}; rotational relaxation 2_{21}–1_{10}).

The rotational populations deviate strongly from LTE (Table 4). Collisional effects should be most significant for the low-lying energy states, yet there is no evidence to support collisional equilibration for those levels (for example, 2_{21}, 2_{12}). The excitation temperature for 2_{21} relative to 1_{01} cannot exceed 70 K, for example. Furthermore, the absence of lines originating from levels with $J > 2$ in our spectral bandpass confirms directly that high J states are not being excited significantly in cometary H_2O. The tentative observations of the 6_{16}–5_{23} transition in two comets continue to defy explanation.

Only three lines of para-H_2O were observed, originating from the three lowest levels of 001. The fluorescence equilibrium equations for the levels 2_{12} and 1_{10} of 001 show that the population of 2_{11} relative to 1_{11} is less than 25 percent and is consistent with 0 percent. By neglecting the population in 2_{11}, these two equations can be rewritten to include pumping from 3_{13}. The solution then demonstrates that the population of 3_{13} is less than 28 percent, with a probable value of ~10 percent, relative to 1_{11}.

The iterative approach taken above is somewhat risky but at least yields no internal inconsistencies at the 30 percent level. In any event, the above results and the absence of any high J lines in our spectrum, indicate that there is no strong excitation of high J levels in para-H_2O, which is consistent with the results obtained for ortho-H_2O. If we neglect the population of all states except 1_{11} and 0_{00} (possibly a riskier assumption than those made above), then the steady-state equations of 2_{12}, 1_{10}, and 1_{01} can be used to solve for the populations of 1_{11} relative to 0_{00} (Table 4, model C). We obtain the value 0.79 ± 0.06, corresponding to an excitation temperature of ~40 K.

The model used here is inadequate in many respects, but it does demonstrate the highly non-LTE excitation conditions of H_2O in a cometary coma, thereby validating the most important features predicted in recent models (*22, 23, 25*). A different approach, in which a detailed physical model of the coma is used to synthesize the cometary spectrum for comparison with the measured intensities, remains to be described.

Summary and implications for cometary science. We have reported the first definite detection of H_2O in Halley's comet, and the first interpretable and unequivocal detection for any comet. We present our initial findings on its production rate, and on the radiative and collisional environment in the coma. The identifications and intensities of observed spectral lines largely confirm predictions based on nonthermal equilibrium physical models. The observed ortho-para ratio is consistent with extremely low nuclear spin temperatures, suggesting that the observed H_2O may have vaporized directly from the ice phase. The many insights provided into the physical and chemical properties of the inner coma illustrate the high information content of high resolution infrared spectra.

The definitive detection of cometary H_2O may mark the beginning of a new era in cometary science. We have used high resolution infrared spectroscopy of cometary infrared resonance fluorescence radiation to determine the presence of a major volatile (H_2O) in a cometary coma and, by inference, in a cometary nucleus. This approach represents an effective way for studying the volatile fraction of cometary nuclei by remote means.

REFERENCES AND NOTES

1. F. L. Whipple, *Astrophys. J.* **111**, 375 (1950); *ibid.* **113**, 464 (1951). A comprehensive modern review of comets is L. Wilkening, Ed., *Comets* (Univ. of Arizona Press, Tucson, 1982).
2. R. L. Newburn and D. K. Yeomans, *Annu. Rev. Earth Planetary Sci.* **10**, 297 (1982).
3. M. H. Moore, B. Donn, R. Khanna, M. F. A'Hearn, *Icarus* **54**, 388 (1983).
4. J. M. Greenberg, in *Comets*, L. Wilkening, Ed. (Univ. of Arizona Press, Tucson, 1982), p. 131.
5. J. S. Lewis and R. G. Prinn, *Astrophys. J.* **238**, 357 (1980).
6. A. Delsemme, in *Comets*, L. Wilkening, Ed. (Univ. of Arizona Press, Tucson, 1982), p. 85.
7. H. Campins, G. H. Rieke, M. J. Lebofsky, *Nature (London)* **301**, 405 (1983).
8. M. S. Hanner, *Astrophys. J.* **277**, L75 (1984).
9. M. F. A'Hearn, E. Dwek, A. T. Tokunaga, *ibid.* **282**, 803 (1984).
10. H. A. Weaver, P. D. Feldman, M. C. Festou, M. F. A'Hearn, *ibid.* **251**, 809 (1981); ——, H. U. Keller, *Icarus* **47**, 449 (1981). For a review of ultraviolet observations of comets, see P. D. Feldman, in *Comets*, L. Wilkening, Ed. (Univ. of Arizona Press, Tucson, 1982), p. 461.
11. For recent reviews of radio OH observations of comets, see F. P. Schloerb and E. Gerard, *Astron. J.* **90**, 1117 (1985); L. E. Snyder, *ibid.* **91**, 163 (1986).
12. G. Herzberg and H. Lew, *Astron. Astrophys.* **31**, 123 (1974).
13. K. W. Ogilvie, M. A. Coplan, P. Buchsler, J. Geiss, *Science* **232**, 374 (1986).
14. W. M. Jackson, T. Clark, B. Donn, in *The Study of Comets*, B. Donn, M. Mumma, W. Jackson, M. A'Hearn, R. Harrington, Eds. (NASA SP-393, Washington, DC, 1976), part I, p. 272.
15. W. J. Altenhoff *et al.*, *Astron. Astrophys.* **125**, L19 (1983).
16. For a review of radio results, see L. E. Snyder, *Icarus* **51**, 1 (1982).
17. A. E. Roche, C. B. Cosmovici, S. Drapatz, K. W. Michel, W. C. Wells, *ibid.* **24**, 120 (1975).
18. M. J. Mumma, T. Kostiuk, S. Cohen, D. Buhl, P. C. von Thuna, *Nature (London)* **253**, 514 (1975).
19. J. R. Johnson, U. Fink, H. P. Larson, *Astrophys. J.* **270**, 769 (1983).
20. M. J. Mumma, in *Vibrational-Rotational Spectroscopy for Planetary Atmospheres*, M. J. Mumma, K. Fox, J. Hornstein, Eds. (NASA CP-2223, Washington, DC, 1982), vol. 2, p. 717.
21. Th. Encrenaz, J. Crovisier, M. Combes, J. F. Crifo, *Icarus* **51**, 660 (1982); T. Yamamoto, *Astron. Astrophys.* **109**, 326 (1982).
22. H. A. Weaver and M. J. Mumma, *Astrophys. J.* **226**, 782 (1984).
23. J. Crovisier, *Astron. Astrophys.* **130**, 361 (1984).
24. T. Y. Brooke, T. R. Geballe, R. F. Knacke, K. S. Noll, A. T. Tokunaga, *IAU Circ. 4151* (1985).
25. D. Bockelee-Morvan and J. Crovisier, Proceedings of "Asteroids, Comets, Meteors II" (Uppsala, 3 to 6 June 1985), in press.
26. D. S. Davis, H. P. Larson, M. Williams, G. Michel, P. Connes, *Appl. Optics* **19**, 4138 (1980).
27. The spectroscopy of H_2O is discussed in G. Herzberg, *Molecular Spectra and Molecular Structure*, vol. 2, *Infrared and Raman Spectra of Polyatomic Molecules* (Van Nostrand, New York, 1945).
28. Branching ratios were calculated from line intensities given in *Water Vapour Line Parameters from Microwave to Medium Infrared*, by J. M. Flaud, C. Camy-Peyret, and R. A. Toth (vol. 19 of International Tables of Selected Constants Series, Pergamon, Oxford, 1981); also R. A. Toth, private communication.
29. We used the ground-based magnitude (7.1) at K band (2.2 μm) measured on 25.05 December 1985 UT by E. P. Ney and A. G. Knutson [*IAU Circ. 4161* (1986)] to derive an estimated specific intensity of $\sim 1.3 \times 10^{-12}$ W cm^{-2} sr^{-1} cm^{-1} for the continuum in our beam, assuming a ρ^{-1} brightness distribution (ρ = projected slant distance to the nucleus). We took the 2.65-μm continuum level to be approximately equal to the 2.2-μm level.
30. A. Farkas, *Ortho-hydrogen, Para-hydrogen, and Heavy Hydrogen* (Cambridge Univ. Press, Cambridge, England, 1935); H. P. Hopkins, Jr., R. F. Curl, Jr., K. J. Pitzer, *J. Chem. Phys.* **48**, 2959 (1968).
31. M. J. Mumma, unpublished data. J. Crovisier has independently recognized the importance of the ortho-para ratio [private communication, 1986; see also (*23*)].
32. C. Camy-Peyret, J. M. Flaud, G. Guelachvili, C. Amiot, *Mol. Phys.* **26**, 825 (1973); see also (*28*).

33. We thank the manager, Louis Haughney, of the NASA-Kuiper Airborne Observatory and the support staff for their contributions to the success of this investigation. We thank Fred Espenak for ephemeris support and Donald K. Yeomans for providing updated cometary elements. Supported by the NASA Astrophysics Division by grants NAG 2-356 to the Johns Hopkins University and NAG 2-206 to the Lunar and Planetary Laboratory (University of Arizona) and by RTOP's 188-41-55, 196-41-54, and 352-02-03 to NASA Goddard Space Flight Center.

3 March 1986; accepted 5 May 1986